

SLAC-PUB-12425
IPBI TN-2007-1
28 March 2007

Proposal to modify the polarimeter chicane in the ILC 14 mrad extraction line

**Ken Moffeit, Takashi Maruyama, Yuri Nosochkov, Andrei Seryi,
Mark Woodley and Mike Woods**
SLAC

William P. Oliver
Tufts University

Abstract

A proposal is presented in this paper to modify the extraction line polarimeter chicane to allow the Compton backscattered electrons to be deflected further from the beam line, and to provide optics for the downstream GAMCAL detector.

1. Introduction

The current version of the extraction line polarimeter chicane as shown in figure 1 has four magnets located between $z = 120$ to 175 m [1]. We propose to run the last two polarimeter magnets BVEX3P and BVEX4P at $1\frac{1}{2}$ the B-field of the first two magnets BVEX1P and BVEX2P. With the higher field the Compton electrons are deflected further away from the beam line allowing the Cherenkov detector to cover a larger range of the Compton scattered spectrum. Two additional magnets downstream of the polarimeter chicane close the orbit of the extracted beam for transport to the dump. These magnets will be used by the Gamma Calorimeter (GAMCAL) detector [2].

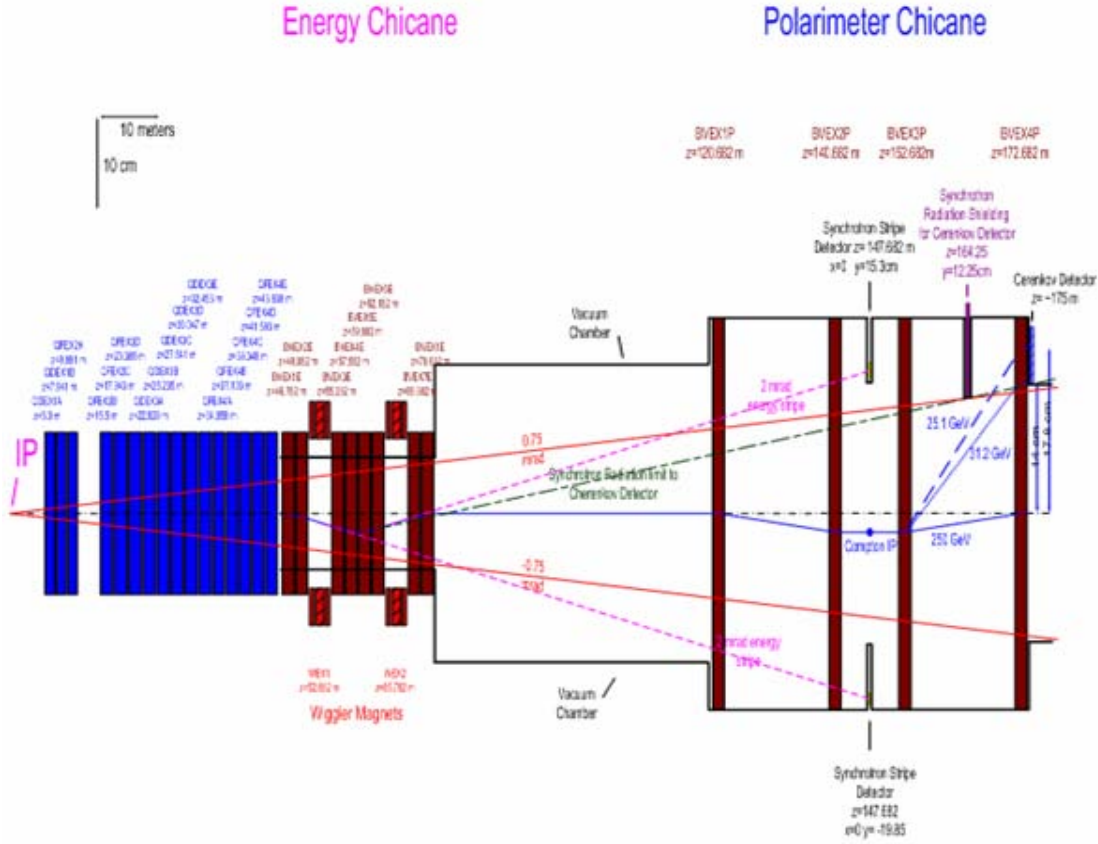


Figure 1: Diagram of the original version of the 14 mrad extraction line showing the energy and polarimeter chicanes. Longitudinal distances are given from the IP. Also shown is the 0.75 mrad beam stay clear from the IP.

2. Status of the 14 mrad extraction optics

Optics of the 14 mrad extraction line [1] has been recently updated to adapt to a push-pull configuration in order to facilitate a rapid exchange of two detectors at the shared e^+e^- Interaction Point (IP). This option requires that the final focus superconducting (SC) magnets inside the detector belong to an independent cryostat separated by a warm section from the outside SC magnets. This dedicated warm section will be used to set-up a convenient break point for detachment and movement of the complete detector with the inside SC magnets in and out of the IP.

To adapt to this configuration, the three original extraction SC quadrupoles [1] are replaced by two shorter quadrupoles placed 5.5 m and 8.51 m from the IP, inside the proposed separate cryostats [3]. The space between these quadrupoles is sufficient for the push-pull warm section. The resultant reduction in the SC quadrupole length is compensated by a higher field gradient which was originally reserved for 500 GeV beam energy upgrade. Consequently, the updated SC extraction quadrupoles are limited to 250

GeV beam energy, while the warm extraction magnets are compatible with up to 500 GeV. The beam apertures of the two SC quadrupoles are set to the maximum values of 15 mm and 26 mm, limited by the separation between the incoming and extraction lines. Longitudinal positions of the downstream extraction magnets are kept the same in this update, and the quadrupole fields are slightly adjusted to maintain the beam focus at the Compton interaction point, 147.682 m downstream of IP, and the value of the horizontal angular transformation term of $R_{22} = -0.5$.

The updated optics includes the new system of horizontal and vertical sweeping kickers placed downstream of the polarimeter chicane and about 100 m before the dump. These kickers will utilize a high frequency modulated horizontal and vertical fields to sweep the beam position on a $R = 3$ cm circle at the dump window in order to increase the effective beam area and thus prevent water boiling in the dump vessel. The extra benefit of this system is that it allowed reducing the length of the extraction line from 400 m to 300 m.

Two new protection collimators are included in the diagnostic chicanes. The 1st collimator is placed at center of the energy chicane, 59.8 m after the IP, where momentum dispersion is 17 mm. Its 40 mm vertical aperture on the low energy side of the beam is set to remove the low energy tail particles with relative energies below 30% - 35%. The 2nd collimator is placed 160 m after the IP, inside the polarimeter chicane, to protect the Cherenkov detector from synchrotron radiation created in the energy chicane bends.

The extraction aperture is maintained large enough for transmission of beamstrahlung photons with up to ± 0.75 mrad angles at the IP and the primary charged particles with energies above 40% of the nominal 250 GeV. A special configuration of beam pipe aperture in the diagnostic region will be shown in the next section.

The above optics modifications do not significantly change the total beam loss in the extraction line, however, the two new chicane collimators help to localize the losses and reduce the load on the extraction magnets. DIMAD tracking of disrupted 250 GeV beam showed that in the nominal ILC parameter option “cs11” [4] the expected primary loss is very small: well below 1 W/m. In the alternative low beam power option “cs14”, where the beam disruption is larger, the power loss on magnets and beam pipe is still quite moderate: within 5 W/m as shown in Figure 2. In this case, the significant power of the lost beam is absorbed by the two new chicane collimators (two red lines in Figure 2) and by the three dump collimators located further downstream.

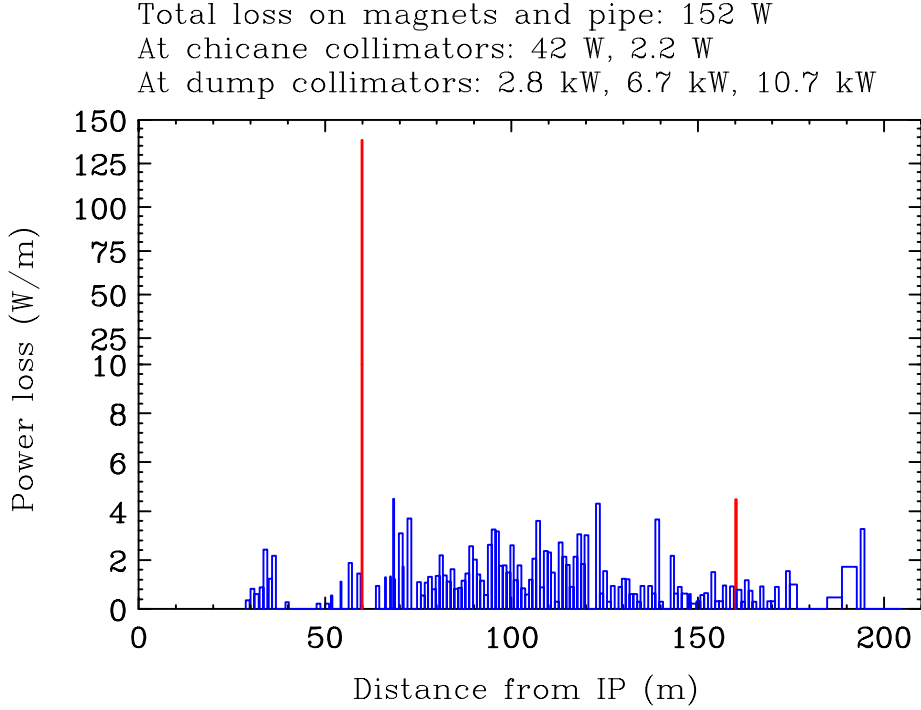


Figure 2: Longitudinal density of the primary beam loss for the ILC low beam power parameter option “cs14” at 250 GeV beam energy. The two red lines show loss on the energy and polarimeter chicane collimators.

The proposed modifications for the polarimeter chicane bends and the additional two bends for GAMCAL detector will be discussed in detail in the next section. The optical β functions and vertical dispersion in the complete extraction line from IP to the dump, including the proposed modifications, are shown in Figure 3. The updated parameters of extraction quadrupoles and the existing and proposed chicane bends are listed in Tables 1 and 2, where L is the magnet length, G is the quadrupole field gradient, R is the aperture radius to beam pipe, and B is the bending field for 250 GeV beam energy. It is required that the warm quadrupoles and energy chicane bends are designed for twice the field in Tables 1 and 2 to be compatible with the 500 GeV beam upgrade.

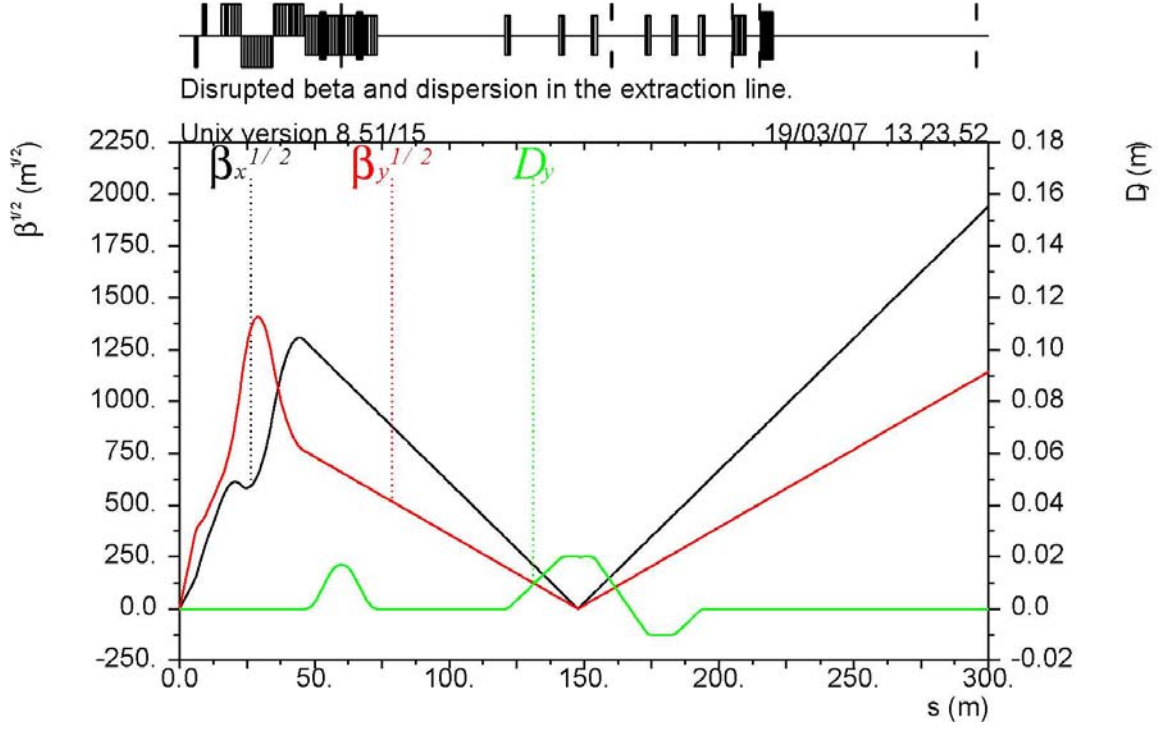


Figure 3: Optical β functions and vertical momentum dispersion D_y in the 14 mrad extraction line from IP to the dump, shown for the 250 GeV nominal disrupted beam.

Table 1: Parameters of the extraction quadrupoles at 250 GeV.

Quad name	Qty	L (m)	G (T/m)	R (mm)
QDEX1 (SC)	1	1.060	100.00	15
QFEX2A (SC)	1	1.200	23.08	26
QFEX2B,C,D	3	2.143	11.19	42
QDEX3A,B	2	2.106	11.93	42
QDEX3C	1	2.106	10.89	46
QDEX3D	1	2.106	9.63	52
QDEX3E	1	2.106	8.08	62
QFEX4A	1	1.945	7.11	71
QFEX4B,C,D,E	4	1.945	5.94	85

Table 2: Parameters of the existing and proposed chicane bends at 250 GeV.

Bend name	Qty	L (m)	B (T)	Half-gap (mm)	Diagnostics
BVEX1E,2E,...,8E	8	2.0	0.4170	85	Energy
BVEX1P,2P	2	2.0	0.4170	117	Polarimeter
BVEX3P	1	2.0	0.6254	117	
BVEX4P	1	2.0	0.6254	132	
BVEX1G,2G	2	2.0	0.4170	147	GAMCAL

3. Proposal to modify the polarimeter chicane

Figure 1 shows the schematic of the original extraction line (before the update), where the beam after the e^+e^- collision first enters the extraction quadrupoles (blue boxes) and then the vertical chicanes for measuring the beam energy and polarization. The quadrupoles focus the primary beam at the Compton IP located at the center of the polarimeter chicane 147.682 meters downstream of the e^+e^- IP. The Compton scattered electrons from the Compton IP traverse magnets 3 and 4 of the polarimeter chicane where they are deflected away from and returned parallel to the beam line. Backscattered Compton electrons of energy 25.2 GeV are 17.8 cm from the beam line at the location of the Cherenkov detector, $z = 175\text{m}$. The beam stay clear is ± 0.75 mrad to accommodate the beamstrahlung photons and disrupted beam after the e^+e^- interactions. This means that the beam pipe radius must be larger than 13.125 cm at the Compton detector plane. After allowing for synchrotron radiation from the energy chicane magnets the first cell of the Cherenkov detector could start at 14 cm corresponding to 31.2 GeV. This allows space for only four 1 cm cells between the 31.2 GeV electrons and the 25.2 GeV backscattered electrons.

We propose to run magnets BVEX3P and BVEX4P of the polarimeter chicane at $1\frac{1}{2}$ the field strength of magnets BVEX1P and BVEX2P. Two additional magnets (BVEX1G and BVEX2G) with the same field strength as magnets BVEX1P and BVEX2P return the beam to the center beam line and bring the dispersion back to zero as shown in Figure 3 (green line). Figure 4 shows the updated magnet configuration and the proposed modification to the extraction polarimeter chicane. As seen in Figure 5 the Compton backscattered electrons are now 27.7 cm above the beam line. The Cherenkov cell closest to the beam pipe begins at 15 cm and corresponds to Compton scattered electrons of 44 GeV. This configuration allows thirteen 1 cm cells between Compton scattered electrons of 44 GeV and 25.2 GeV.

The target for the Gamma Calorimeter will be located in the 8 m drift between magnets BVEX1G and BVEX2G. The detector for the Gamma Calorimeter will be located outside the beam stay clear in the reserved 10 m drift downstream of the magnet BVEX2G between $z = 195\text{ m}$ and 205 m [2].

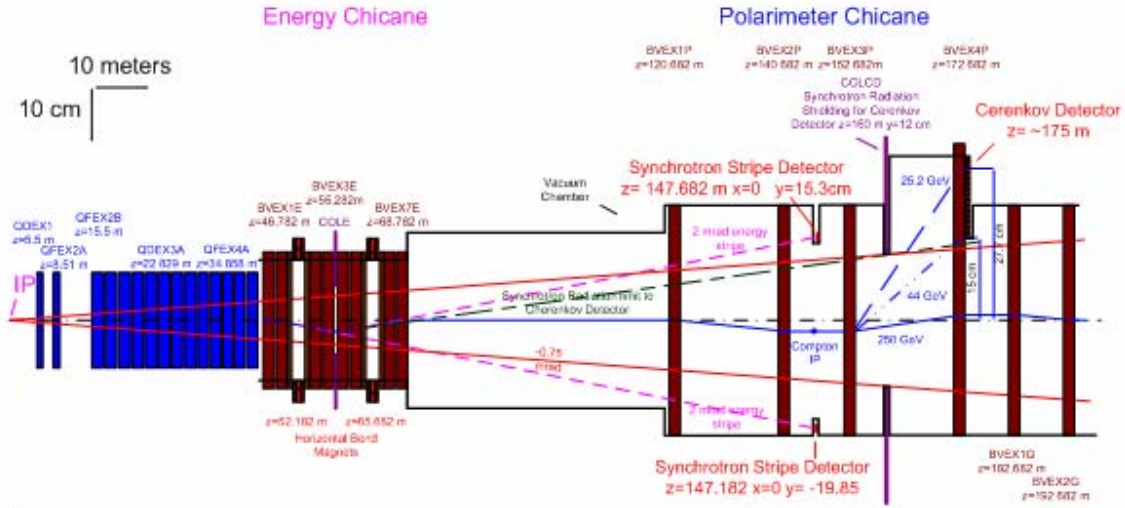


Figure 4: Diagram of the Energy Chicane and Polarimeter Chicane in the proposed modified 14 mrad extraction line showing the four magnet polarimeter chicane with additional two magnets for GAMCAL.

Polarimeter Chicane

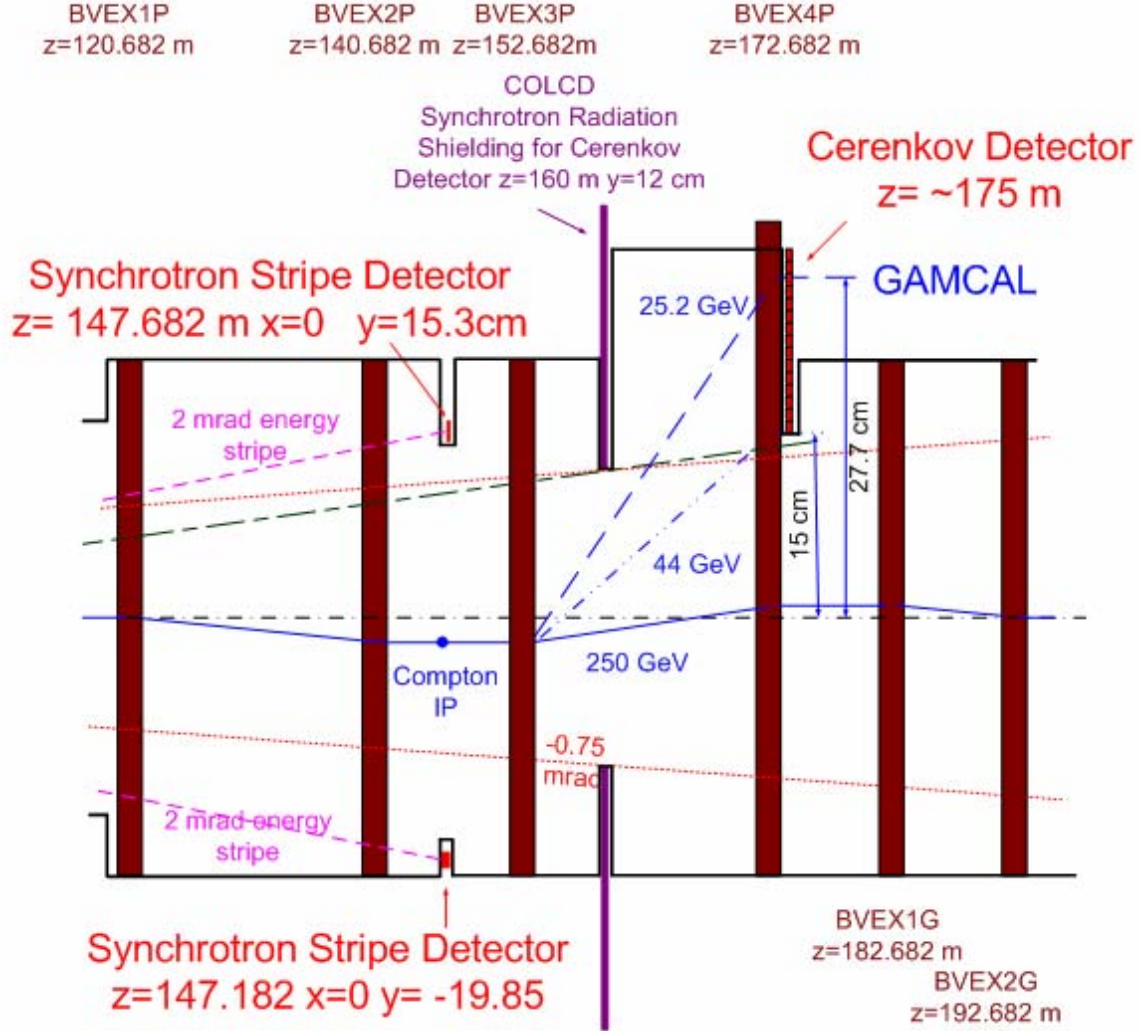


Figure 5: Details of the Polarimeter Chicane in the modified 14 mrad extraction line showing the proposed four magnet chicane. The additional two magnets (BVEX1G and BVEX2G) close the orbit. The Gamma Calorimeter target will be located between the last two magnets and the detector placed after the last magnet in the reserved 10 m drift.

4. Beam studies

Simulated disrupted beams from e^+e^- collisions for the ILC were transported using GEANT [5] in the modified 14 mrad extraction line. A MAD SURVEY file of the extraction beam optics was used to model the magnet locations, strengths, and orientations in GEANT. Particle interactions are simulated in GEANT, and the secondary

particles are transported through the extraction line. Magnets apertures, collimators and the beam pipe are simulated. Distributions of positions, energy and angles at the Compton Detector Plane are shown. Previous studies of the 14 mrad extraction line are found in reference [6]. Disrupted beam distributions were generated using Guinea-Pig code [4]. For these studies option cs11 corresponds to the nominal ILC beam (mean energy 244.1 GeV and RMS 10.98 GeV) and option cs14 with parameters set for Low Beam Power (234.6 GeV and RMS 22.10 GeV). The e^+e^- collision in the Low Power parameter option gives a larger beam disruption resulting in broader energy and angular distributions.

Figure 6 shows a plot generated by GEANT giving the magnets and ray traces for 100 beam particles from parameter set cs11. The dispersion at the Compton IP for a 250 GeV beam is 2 cm. The drawings at the top of the figure are for the extraction line before update and the ones at the bottom are for the modified extraction line.

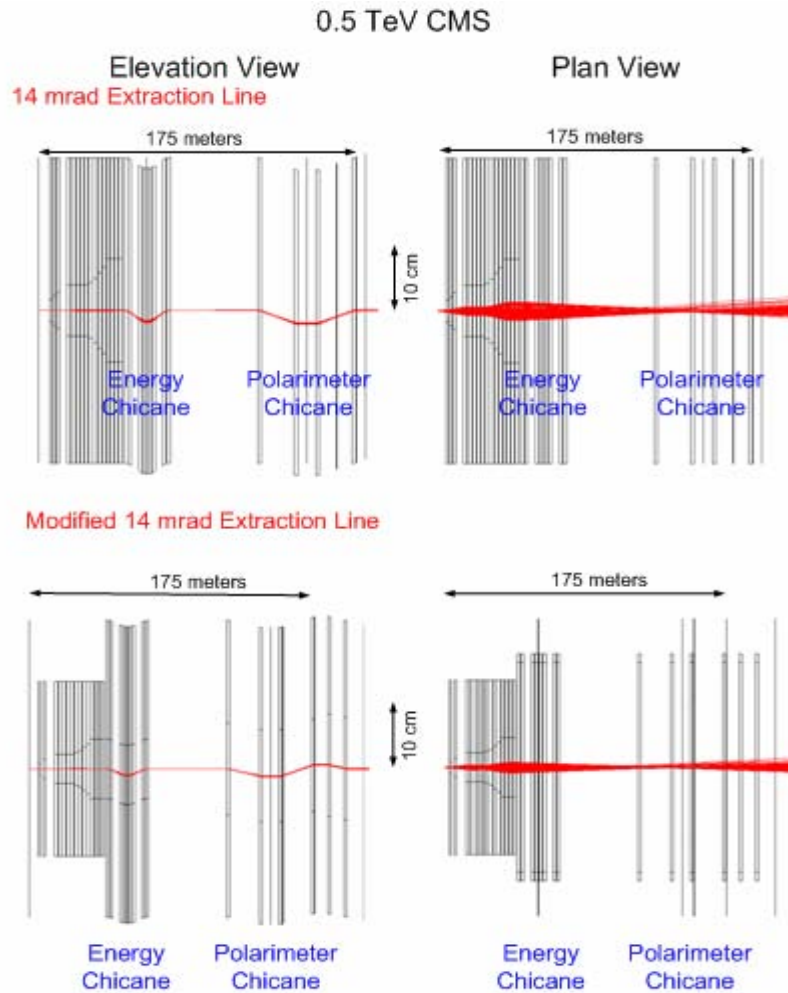


Figure 6: GEANT generated drawing of the beam line elements with 100 beam tracks shown. The drawings at the top of the figure are for the extraction line before update and the ones at the bottom are for the modified extraction line.

Compton scattered electrons are generated in GEANT at the Compton IP from the interaction of the extracted beam on 2.33 eV laser light. In this study every beam track that reaches the Compton IP is converted into a Compton scattered electron. Figure 7 shows a plot of ray traces for 100 beam particles and Compton electrons generated at the Compton IP. The distributions in energy and the vertical position, y , of the Compton scattered electrons at the Compton detector plane are shown in Figure 8 for $y > 14$ cm. The backscattered electrons have energy of 25.2 GeV and enter the Compton detector at 27.7 cm.

Modified 14 mrad Extraction Line

0.5 TeV CMS

Elevation View

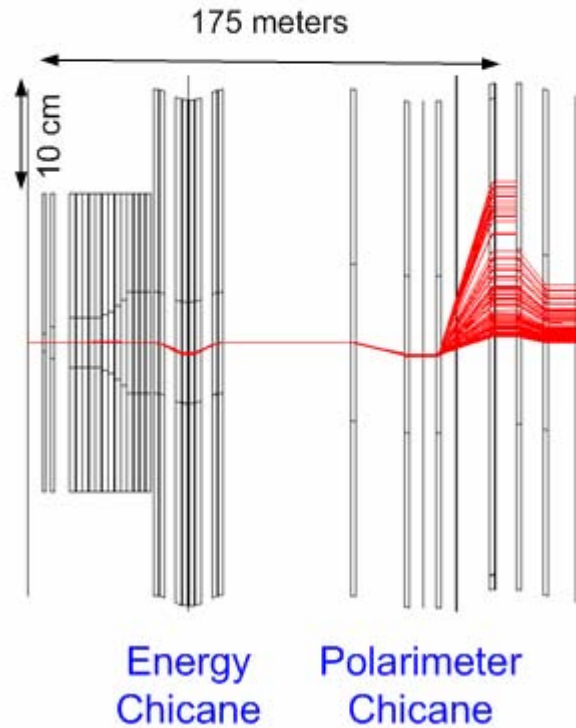


Figure 7: GEANT generated drawing of the beam line elements with 100 beam tracks shown. At the Compton IP each beam track is changed into a Compton scattered electron. The Compton scattered electrons with low enough energy to exit the beam pipe are detected in the Compton Cherenkov detector located at $z = 175$ m.

Compton scattered electrons at the
Compton detector plane
 $z=175\text{m}$

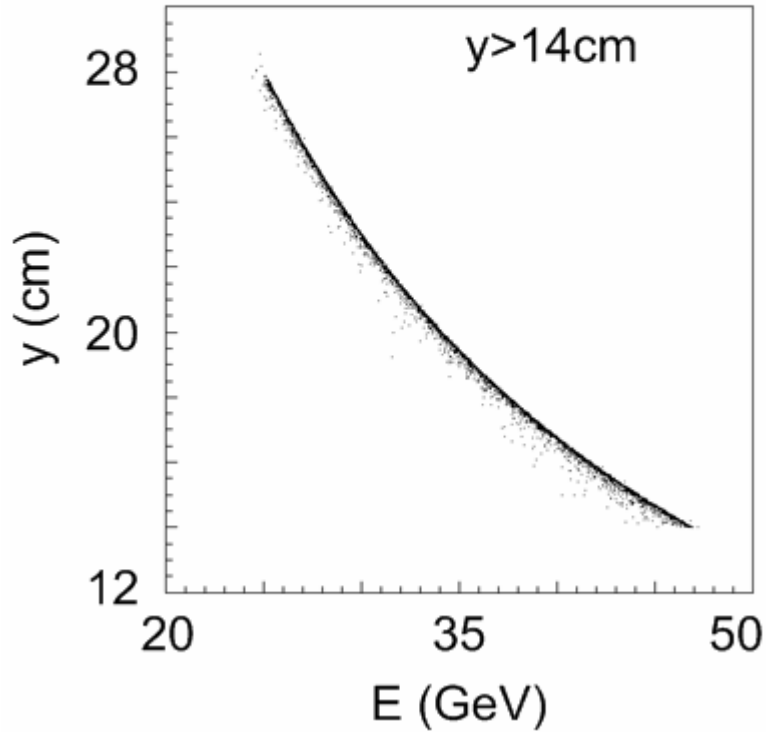


Figure 8: Energy versus y for the Compton scattered electrons at the Compton Detector plane ($z = 175\text{m}$).

A Cherenkov cell width of $\sim 1\text{ cm}$ will allow most of the Compton electrons to enter the detector as seen in Figure 9 where x versus y is plotted. Energy histograms for different y -selections are shown in Figure 10. One centimeter vertical cell size is planned. The distributions on the left of Figure 10 are near the backscattered electron position at the Cherenkov detector, and those near the beam pipe at $y = 15\text{ cm}$ are close to 90° degrees in the center of mass system of the laser light and beam electron scattering angle. Near the backscattered electron energy of 25.2 GeV the 1 cm high Cherenkov cell will accept approximately 1 GeV . Near the beam pipe the 1 cm cell will accept about 2.5 GeV (from $\sim 44\text{ GeV}$ to $\sim 41.5\text{ GeV}$).

Compton scattered electrons at the
Compton detector plane
 $z=175\text{m}$

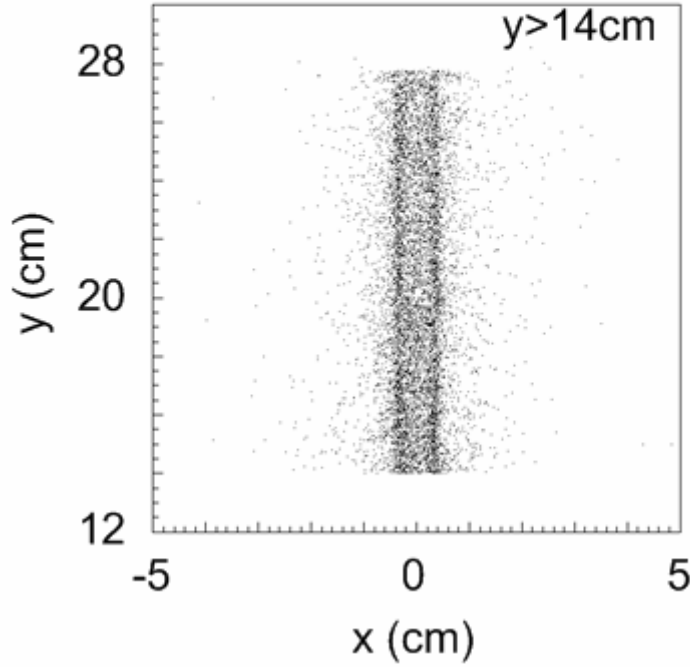


Figure 9: Distribution of x versus y for Compton scattered electrons at the Compton Detector plane ($z = 175\text{ m}$).

For each of the studied beam parameter options, cs11 and cs14, two sets of disrupted electron distributions were used in tracking. The first data set contains $\sim 35 \cdot 10^3$ electrons simulating the full beam distribution. This set is sufficient to study the properties of the full disrupted beam in the extraction line. However, it does not have enough particles for accurate beam loss calculation. Since the extraction losses occur only for electrons with very low energies and large angles, the second data set contains only the beam tail particles with energies below 65% of the nominal 250 GeV and/or x - y angles at IP exceeding 0.5 mrad. This “tail” data set is extracted from $\sim 17.5 \cdot 10^6$ particles in the full generated beam to provide a much higher beam tail statistics for the beam loss calculation.

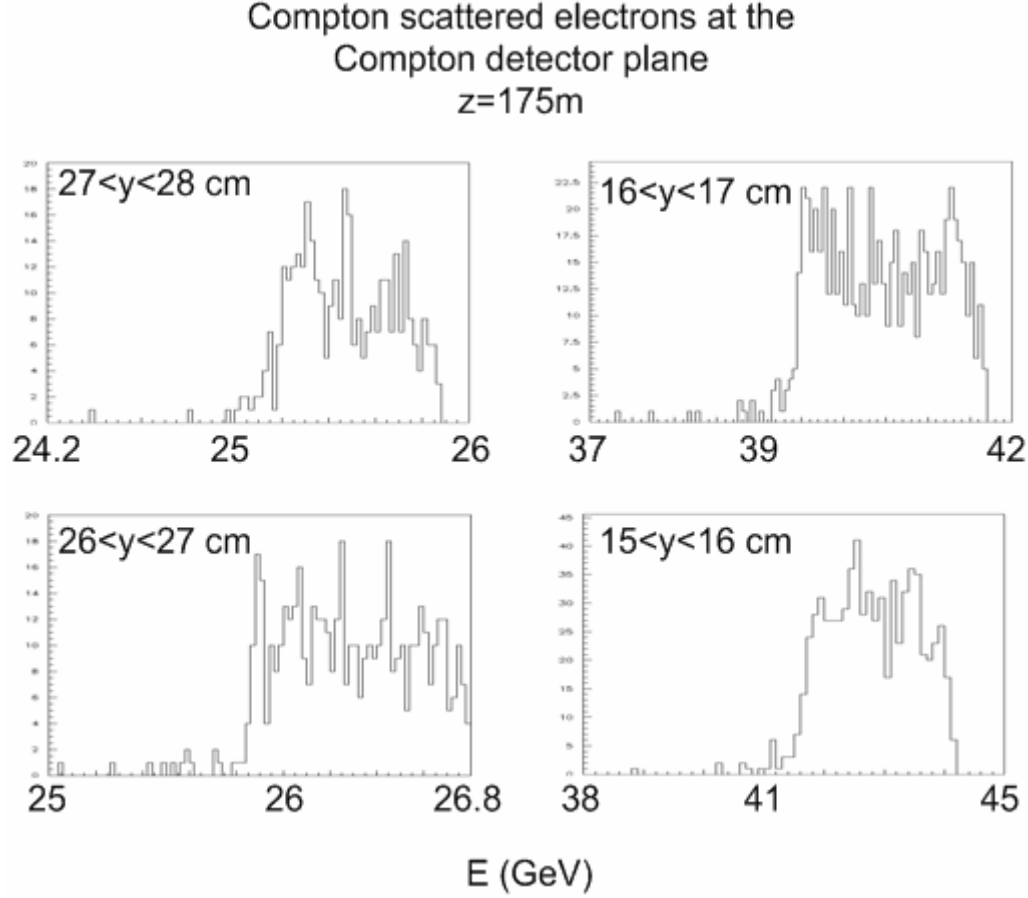


Figure 10: Energy distribution for Compton scattered electrons for different selections in y .

Figure 11 shows the x vs y distribution for the extracted beam at three positions in the extraction line. No particles are lost from the 34883 beam particles from the nominal beam option cs11 between the e^+e^- interaction point and the end of the six-magnet polarimeter chicane at $z = 195 \text{ m}$. There are no background particles above $y = 4 \text{ cm}$. The first cell of the Compton Cherenkov detector begins at $y = 15 \text{ cm}$. No beam tail particles with energy less than 65% and/or x - y angles $> 0.5 \text{ mrad}$ were lost between the IP and $z = 195 \text{ m}$ from the total $17.59 \cdot 10^6$ beam particles in the nominal parameter option cs11. The proposed modified six-magnet chicane transports the nominal ILC beam as efficient as the original design.

The low power data set cs14 has 5 beam tracks lost from 34913 between the e^+e^- IP and $z = 195 \text{ m}$ (0.014%). No particles in this sample are lost between the Compton detector plane and $z = 195 \text{ m}$. The number of lost particles before the Compton detector is similar in the original and modified extraction line designs. The distribution at the Compton Detector plane is broader from the low power data set, but, there are no particles above $y = 8 \text{ cm}$ from the 34913 beam particles.

The low energy tail of the disrupted beam in the low power option cs14 was also studied corresponding to total $17.45 \cdot 10^6$ beam particles. There are 0.0096% lost particles between the e^+e^- IP and the Compton detector plane (an additional 0.00005% are lost between the Compton detector plane and $z = 195$ m). The lost particles produce backgrounds at the Compton detector of photons and charged particles. Extrapolating to a beam of $2 \cdot 10^{10}$ particles the backgrounds would be ~ 1650 per centimeter squared (the area of a Cherenkov cell). Most of this background is photons and only a small portion will convert to e^+e^- pairs in the material before the Cherenkov detector. In addition, 56% of the background particles are photons of energy less than 15 MeV and will not give Cherenkov light. The backscattered electron counting rate is high for the proposed Compton Polarimeter with about 650 Compton electrons per GeV at the endpoint energy of 25.2 GeV [7]. Therefore the backgrounds from secondary interactions should be small compared to the signal even for Low Power beam parameter running.

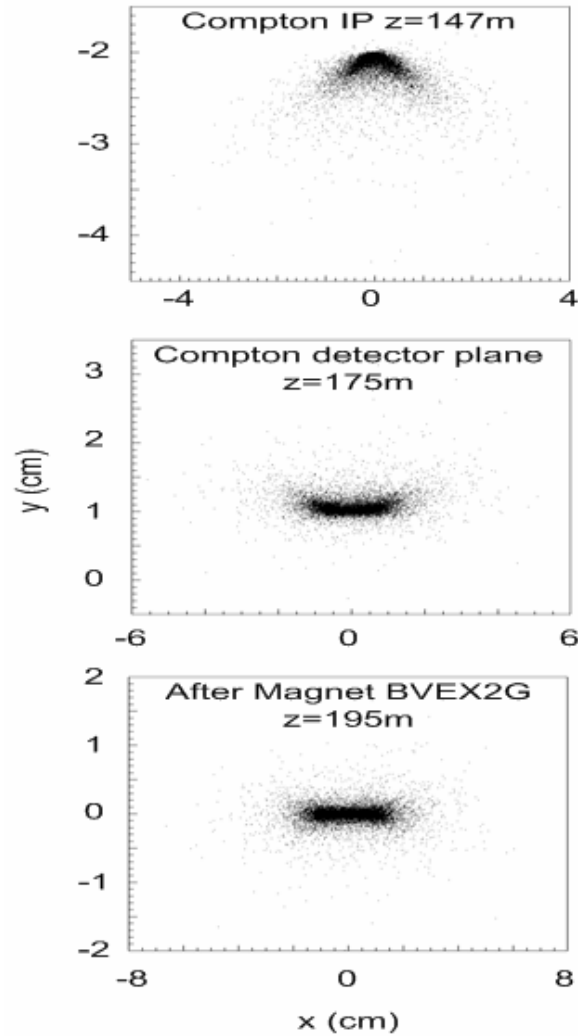


Figure 11: Distribution of x vs y for the extracted beam electrons at the Compton IP, the Compton detector plane and at the end of magnet BVEX2G.

At the end of the proposed six magnet polarimeter chicane the beam is well behaved and centered on the central beam line of $x = 0$ and $y = 0$ with an x-rms of 7.7 mm (x angle-rms = 0.12 mrad) and y-rms 0.89 mm (y angle-rms = 0.0072 mrad).

The synchrotron radiation at the Compton detector plane is given in Figure 12. The sharp cutoff at 14 cm is the shadow from the special collimator located at $z = 160$ m shown in Figures 4 and 5. There are no synchrotron radiation photons above 14.04 cm.

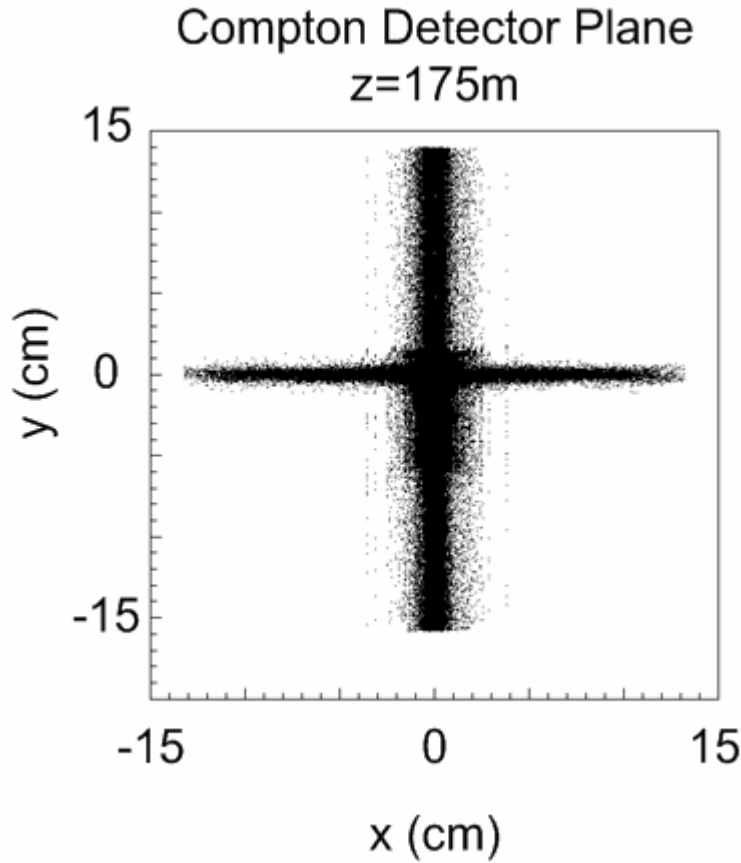


Figure 12: Distribution of x vs y at the Compton detector plane for synchrotron radiation photons generated from the upstream magnets.

5. Conclusions

The proposed modified extraction line with two additional magnets improves the acceptance of the Compton scattered electrons allowing detection over a larger part of the Compton electron energy spectra. The backscattered electrons are further away from the beam pipe by ~ 10 cm. The beam transport through the modified extraction line is

efficient. Backgrounds from synchrotron radiation produced upstream of the Cherenkov detector and from lost particles along the beam line are similar to that in the original extraction line design, and will be small compared to the Compton scattered electron signal.

References

- [1] Y. Nosochkov, T. Markiewicz, T. Maruyama, A. Seryi (SLAC), B. Parker (Brookhaven). *ILC Extraction Line for 14 mrad Crossing Angle*. SLAC-PUB-11591, Dec 8, 2005.
- [2] William Morse, *Updates on GamCal*, see <http://www-project.slac.stanford.edu/ilc/acceldev/beamdelivery/>, March 6, 2007.
- [3] B. Parker, see http://www-project.slac.stanford.edu/lc/bdir/Meetings/beamdelivery/2007-01-23/BDS_ir_status_22jan07.pdf, January 22, 2007.
- [4] Andrei Seryi, <http://www.slac.stanford.edu/~seryi/>, November 2005.
- [5] GEANT-3, CERN Program Library Long Write-up W5013, CERN, March 1994.
- [6] Ken Moffeit, Takashi Maruyama, Yuri Nosochkov, Andrei Seryi and Mike Woods (SLAC), William P. Oliver (Tufts University), Eric Torrence (University of Oregon), *Comparison of 2 mrad and 14/20 mrad Crossing Angle Extraction Lines*, SLAC-PUB-11956, July 2006.
- [7] Ken Moffeit and Mike Woods, *Laser System for a Compton Polarimeter*, IPBI TN-2003-2, December 2003, <http://www.slac.stanford.edu/xorg/lcd/ipbi/notes/ComptonLaserSystem.pdf> .